Fixed target Drell-Yan data and NNLO QCD fits of parton distribution functions

Sergey Alekhin

Institute for High Energy Physics Protvino, 142281, Russia

Kirill Melnikov

Department of Physics and Astronomy, University of Hawaii Honolulu, Hawaii, 96822, USA

Frank Petriello

Department of Physics, University of Wisconsin, Madison, Wisconsin 53706, USA

We discuss the influence of fixed-target Drell-Yan data on the extraction of parton distribution functions at next-to-next-to-leading order (NNLO) in QCD. When used in a parton distribution fit, the Drell-Yan (DY) data constrain sea quark distributions at large values of Bjorken x. We find that not all available DY data are useful for improving the precision of parton distribution functions (PDFs) obtained from a fit to the deep inelastic scattering (DIS) data. In particular, some inconsistencies between DIS-based parton distribution functions and DY data for large values of dilepton rapidity are found. However, by selecting a sample of the DY data that is both representative and consistent with the DIS data, we are able to perform a combined PDF fit that significantly improves the precision of nonstrange quark distributions at large values of x. The NNLO QCD corrections to the DY process are crucial for improving the precision. They reduce the uncertainty of the theoretical prediction, making it comparable to the experimental uncertainty in DY cross-sections over a broad range of x.

　　　　　　　　　　　　　　PACS numbers: 13.60.Hb, 12.38.Bx

I. INTRODUCTION

Parton distribution functions (PDFs) are important for the theoretical description of hard QCD processes at hadron colliders. Because of the factorization of short- and long-distance physics, these functions are universal, and once extracted from one process they can be applied to other hard QCD processes. With the Tevatron Run II under way and the LHC upcoming, the need for reliable PDFs is increasing. Particular aspects that warrant careful investigation are PDF uncertainties and their influence on theoretical predictions, and the consistent inclusion of higher order QCD corrections into PDF fits.

The current standard for perturbative calculations in QCD is next-to-leading order (NLO). The typical accuracy of this approximation is 10–15%. While this level of precision is adequate for many physics processes that are studied at the Tevatron and will be studied at the LHC, there are processes for which higher accuracy is required. This may happen for either calibration processes or important discovery channels, such as the production of electroweak gauge bosons, the Higgs boson, heavy quarks, and two jets with large transverse momenta. For such processes, it is desirable to have a theoretical description valid through next-to-next-to-leading order (NNLO) in perturbative QCD. A significant effort is currently under way to develop theoretical tools for computing parton scattering cross-sections with NNLO accuracy. To use those calculations for predicting actual hadronic cross-sections, parton distribution functions with NNLO accuracy are required as well.

There are currently two distinct approaches to extracting PDFs from existing data. The first one is the global fit that is practiced by the MRST [1] and CTEQ [2] collaborations. The data set in this case includes deep inelastic scattering (DIS), Drell-Yan (DY) pair production in fixed target and collider experiments, and Tevatron jet cross-sections. While such an approach benefits from the wealth of data, its drawback is that inconsistent data may influence the quality of the fit. In addition, going beyond the next-to-leading order within this framework is difficult since very few partonic processes are currently known through NNLO in perturbative QCD.

A different approach to extracting PDFs was suggested in [3]. The data set in this case is restricted to deep inelastic scattering. Higher order QCD corrections can be included consistently within this approach since the QCD corrections to DIS coefficient functions and DGLAP splitting functions are known through NNLO [4–6]. The disadvantage of the DIS-based approach is that the DIS data are only sensitive to certain combinations of PDFs. Consequently, not every parton distribution function can be reliably constrained. This leads to large, approximately 20%, errors on sea quark and gluon distributions at relatively large values of the Bjorken variable x, $x \gtrsim 0.1$.

The determination of sea quark distribution functions can be improved if the approach of Ref. [3] is extended to include precise data on fixed-target Drell-Yan processes [7–10]. These data cover the important kinematic range $Q^2 \sim (20 \text{ GeV})^2$ and $x \gtrsim 0.1$, and are strongly sensitive to sea quark distributions in the proton. While such an extension seems obvious, Drell-Yan data was not incorpo-

rated into the NNLO fit of Ref. [3] because until recently only the NLO calculation of the dilepton rapidity distribution in the Drell-Yan process was available [11]. Recent NNLO QCD computations [12,13] of the rapidity distribution remove this obstacle and permit consistent inclusion of the Drell-Yan data in the PDF fit. The purpose of the present paper is to perform a combined analysis of the DIS and DY data and to elucidate the impact of the DY data on parton distribution functions.

This paper is organized as follows. In the next Section we investigate the consistency of fixed-target DY data [7–9] and theoretical predictions obtained with the DIS PDFs of Ref. [3]. This consistency is the necessary condition for combining the DIS and DY data; if it is not fulfilled, the errors on parton distribution functions obtained in a combined fit are meaningless. We show that available DY data are precise enough so that it is beneficial to include these data in a combined DIS/DY fit. Having established the consistency of the DIS PDFs with the DY data, we incorporate those data in a combined DIS/DY fit which is described in Sec. III. Inclusion of the DY data into the fit improves the precision of sea quark distribution functions for large values of x. The quality of the DIS/DY fit is similar to the quality of the DIS fit of Ref. [3]. We discuss implications of the combined fit for basic QCD and electroweak observables such as the value of the strong coupling constant $\alpha_s(M_Z)$, the Pascos-Wolfenstein ratio and the production cross-sections of Z and W bosons at the Tevatron. Finally, we present our conclusions.

II. DIS PARTON DISTRIBUTION FUNCTIONS AND THE DY DATA

As we discussed in the Introduction, before incorporating fixed-target DY data into the PDF fit based on the DIS data, we need to check if those data sets are consistent. To do so, we compute the dilepton rapidity distribution for fixed-target DY processes using the DIS PDFs [3] and compare the results of the calculation to experimental data [7–10]. We assume that dimuon production in the Drell-Yan process is well described by the leading twist factorization and that nuclear corrections are unimportant. There are then two sources of uncertainties in the theoretical prediction. First, there is residual dependence on the factorization and renormalization scales, a feature common to all fixed order calculations in perturbative QCD. Second, parton distribution functions obtained from a fit to data have uncertainties that influence the theoretical prediction of the dimuon rapidity distribution. For the fixed-target DY processes that are considered in this paper, PDF uncertainties are larger than the residual scale uncertainty of the NNLO calculation. We are therefore mostly concerned with PDFs uncertainties in what follows.

We choose three sets of fixed-target DY data for our analysis [7–10]. All experiments use an 800 GeV proton beam but employ different targets such as hydrogen (E-

866), copper (E-605) and deuterium (E-772, E-866). The center-of-mass energy of the DY process for these three experiments is $\sqrt{s} = 38.8$ GeV. These experiments therefore cover a broad range of dilepton invariant mass M and Bjorken x: $M \lesssim 20$ GeV and $x \gtrsim 0.01$. Note that distributions in the Feynman variable x_F rather than the dilepton rapidity are measured by E-772 and E-866; however, the only distribution known through NNLO in perturbative QCD is the dilepton rapidity distribution [12]. We relate the x_F distribution and the rapidity distribution using leading order kinematics. This procedure is justified, since for all DY experiments relevant for our analysis, the average value of the dilepton transverse momentum $p_\perp \sim 1$ GeV is small compared to the dilepton invariant mass $M \gtrsim 5$ GeV. We have checked that the use of leading order kinematics does not introduce significant bias in the final results.

The sensitivity of parton distribution functions to the DY data can be understood from the analytic expression for the DY process at leading order in perturbative QCD. The double differential distribution in dilepton invariant mass M and rapidity Y can be written as

$$\frac{\mathrm{d}^2\sigma}{\mathrm{d}M\mathrm{d}Y} \sim \sum_q q_1(x_1)\bar{q}_2(x_2) + \bar{q}_1(x_1)q_2(x_2), \qquad (1)$$

where $x_1 = M/\sqrt{s}e^Y$ and $x_2 = M/\sqrt{s}e^{-Y}$. Equation (1) implies that, at leading order, the rapidity distribution is determined by either annihilation of a valence quark from the projectile and a sea antiquark from the target or vice versa. Valence and sea quark distribution functions are determined from the DIS data with differing precision. The precision of valence quark distributions is a few percent for all values of x relevant for the DY and DIS data that we consider in this paper. Sea quark distributions are known from the DIS data with a few percent precision only for $x \lesssim 0.1$. For larger values of x the error increases rapidly and exceeds 20% [3]. Since the theoretical predictions for $\mathrm{d}^2\sigma/\mathrm{d}Y\mathrm{d}M$ are more precise than this error [11,12], sea quark distributions can be determined from Eq. (1) with an accuracy comparable to the precision of the available DY fixed-target data.

We begin by comparing theoretical predictions for the dilepton double differential distribution in invariant mass and rapidity with the E-605 proton-copper scattering data. The comparison is shown in Fig. 1 for the rapidity $Y = 0$; note that *different* values of the dilepton invariant mass M contribute to this plot. In the lower panel of Fig. 1, values of x_1 and x_2 are plotted assuming leading order kinematics. Theoretical curves are computed with the NNLO DIS PDFs [3]; we choose equal values for the factorization and renormalization scales and set them equal to the invariant mass of the dilepton pair. The theoretical band reflects the 1σ uncertainty of the DIS PDFs. It is apparent from Fig. 1 that for $x_{1,2} \gtrsim 0.2$, the data are more precise than the theoretical prediction and the data points are
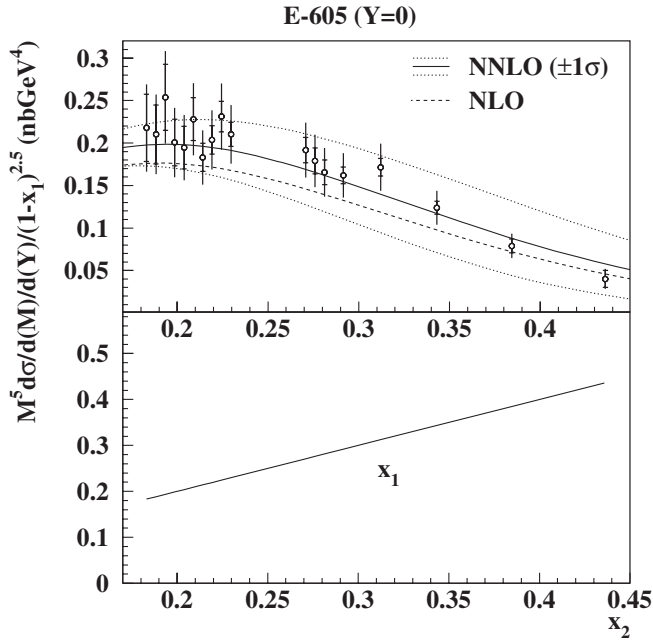
FIG. 1. The NLO (dashes) and NNLO (solid) dilepton rapidity distributions for proton-copper collisions, calculated with the DIS PDFs of Ref. [3], in comparison with the E-605 data at zero rapidity. The NNLO 1σ uncertainty band due to PDF errors is displayed by the dotted curves. The relation between x_1 and x_2 for data points in the upper panel is shown in the lower panel.

within the theoretical uncertainty band. The theoretical prediction shown in Fig. 1 does not include the uncertainty associated with the variation of the renormalization and factorization scales. This uncertainty is about 10% and is much smaller than the 30% PDF error. It is clear from Fig. 1 that the E-605 data are consistent with the DIS data, and may therefore be used in the PDF fit with the DIS data. The precision of the PDFs obtained from a combined fit must improve compared to the situation when only the DIS

data is fitted. We note that although Fig. 1 refers to a particular rapidity value, the E-605 data and the theoretical prediction based on the DIS PDFs are in agreement for other values of dilepton rapidity as well.

A similar analysis can be performed for the E-866 hydrogen and deuterium data; note that the E-866 data covers a broader kinematic range than the E-605 data. In this case, we arrive at two different conclusions depending on the invariant mass of the dilepton pair produced in the DY process. We find that for large dilepton invariant masses there is a reasonable agreement between predictions based on the DIS PDFs and the experimental data; this kinematic region is the same as covered by the E-605 data. However, for small invariant masses and large rapidities the E-866 data are in systematic disagreement with theoretical predictions based on the DIS PDFs. The corresponding results are shown in Fig. 2.

We now discuss the region of small invariant masses in detail. From Fig. 2 we observe that the experimental data is *lower* than the theoretical prediction. The disagreement occurs in the region $x_1 \gg x_2$ with $x_2 \lesssim 0.1$. For such values of $x_{1,2}$, $q_{val}(x_1) \sim q_{val}(x_2)$ and $q_{sea}(x_1) \ll q_{sea}(x_2)$. The second term in Eq. (1) is therefore negligible and the production cross-section is mainly determined by the sea quark distribution $\bar{q}(x_2)$ with $x_2 \lesssim 0.1$. However, for such values of x_2 the precision of sea quark distribution functions obtained from the DIS data is close to a few percent [3]. We therefore conclude that for this kinematic range, the available DY data can not improve the precision of the DIS PDFs. Instead, the theoretical prediction for the dilepton rapidity distribution obtained with the DIS PDFs is a nontrivial check of the consistency of the data. It follows from Fig. 2 that this consistency check fails since the experimental data are systematically below theoretical predictions. We note that the NLO theoretical prediction is in better agreement with the data. While this is clearly accidental, it may result in misleading conclusions about
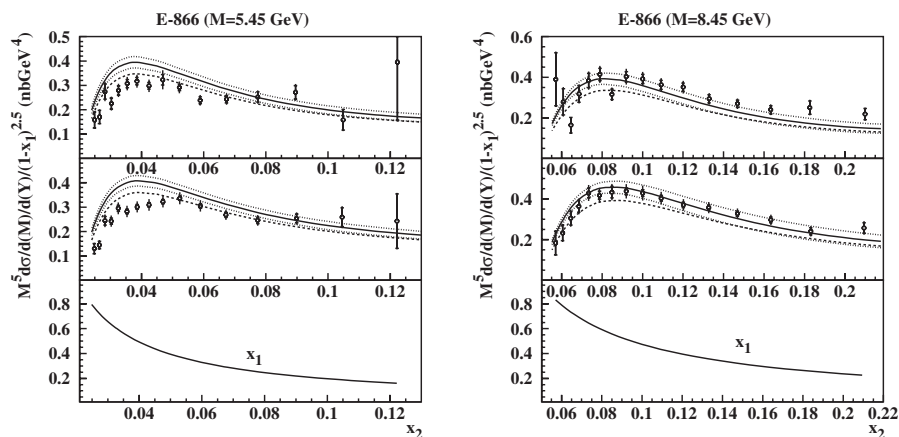
FIG. 2. The same as in Fig. 1 for the E-866 proton (upper panels) and deuteron (middle panels) data for dilepton masses $M = 5.45$ GeV (left panels) and $M = 8.45$ GeV (right panels).

the compatibility of different data sets. Forcing PDFs to fit *both* data sets is a bad solution[1]; the PDFs obtained in that case result in rapidity distribution curves that pass *between* the DIS-based prediction and the E-866 data, the fit quality deteriorates and no reduction of the PDF uncertainty is achieved. We conclude that there is a contradiction between the DIS data and the small dimuon mass data obtained by the E-866 collaboration. In the region where the disagreement occurs, the PDFs are already known precisely from the DIS data. Hence, for such values of dilepton invariant mass the DY data does not improve the precision of sea quark PDFs.

The disagreement between the DIS-based prediction and the E-866 data for small invariant masses occurs at large rapidities. This kinematic region is known to be problematic for existing fixed-target DY experiments. In particular, there is a disagreement between the E-772 and E-866 deuterium data, with the E-772 data points being systematically higher. In principle, this is exactly what is needed to match the DIS-based prediction and the DY data, as can be seen from Fig. 2. However, as shown in Fig. 3, the E-772 data points are somewhat too high on average.

We suspect that problems with the large rapidity region originate from underestimated systematic uncertainties. If this is the case, the ratio of cross-sections for hydrogen and deuterium targets measured by the E-866 collaboration [10] is useful since many systematic uncertainties cancel in the ratio. We note that the theoretical prediction for the ratio is also more precise; for example, the dependence on the factorization and renormalization scales, a 10% effect in the theoretical predictions for individual cross-sections, disappears in the ratio.

The E-866 results for the ratio of deuteron to proton cross-sections and the theoretical prediction based on the DIS PDFs are compared in Fig. 4. In this case, there is an agreement between theory and data for small invariant masses, whereas for larger invariant masses and larger values of Bjorken x, the shape of the DY data differs from the DIS prediction. However, this region is not really problematic for the consistency of the DIS and DY data since it is strongly sensitive to sea quark PDFs for $x \gtrsim 0.1$, where sea quark PDFs obtained from the DIS fit suffer from large uncertainties [3]. Given the large PDF errors in the region of x where the disagreement occurs, we conclude that the E-866 data on the ratio of deuteron to proton cross-sections can be used together with the DIS data without sacrificing the quality of the fit.

Having compared theoretical predictions based on the DIS PDFs with the data on DY processes, we briefly discuss changes that can be expected once the DY data is included in the fit. As an illustration, consider the E-866 data for the dimuon invariant mass $M = 8.45$ GeV, shown in Fig. 2. For larger values of x_2, we observe that for both

---

[1]Note that this is exactly what happens in available global fits.
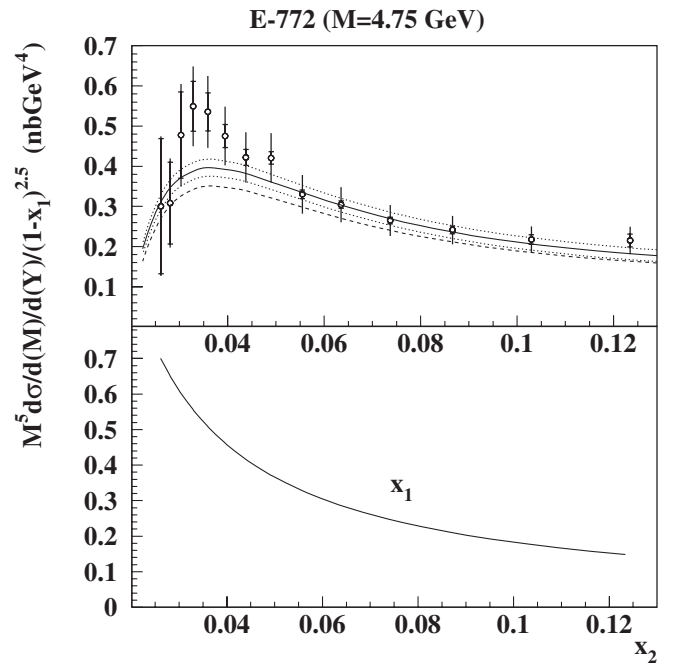
FIG. 3.   Te same as in Fig. 1 for the E-772 deuterium data and for the dimuon invariant mass $M = 4.75$ GeV.

proton and deuteron targets the experimental data points are somewhat higher than the theory prediction. To make theory agree with experiment, we require that sea quark distributions for $x \gtrsim 0.1$ *increase*. Moreover, since the disagreement between theory and experiment is stronger for the proton data, the $\bar{u}$ distribution function should
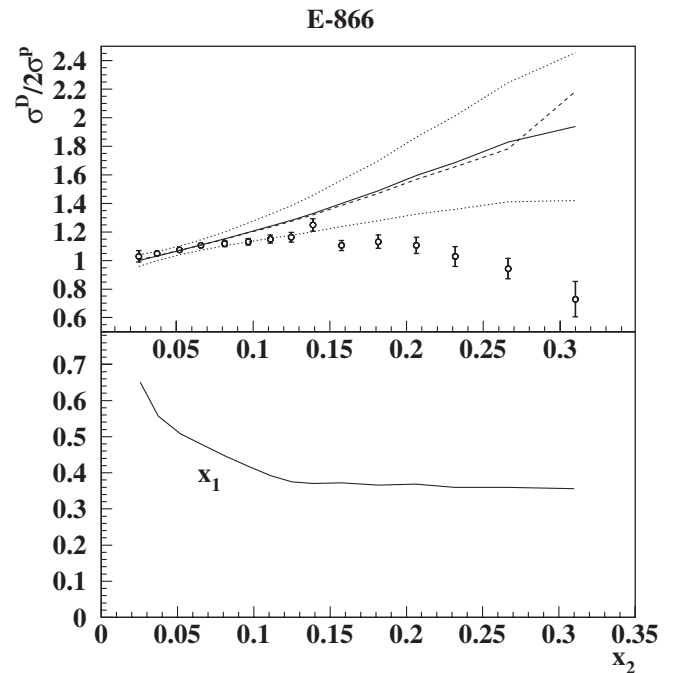
FIG. 4.   The same as in Fig. 1 for the deuteron to proton cross-section ratio measured by the E-886 experiment. Larger values of x_2 correspond to larger dimuon invariant masses.

receive a larger increase than the $\bar{d}$ distribution. This observation is consistent with the results for the ratio of deuteron to proton cross-sections in Fig. 4. The ratio of the two cross-sections can be approximated by

$$\frac{d\sigma(pd)}{2d\sigma(pp)}\bigg|_{x_1 \gg x_2} = \frac{1}{2}\left(1 + \frac{\bar{d}(x_2)}{\bar{u}(x_2)}\right). \tag{2}$$

It follows that since the ratio of *computed* cross-sections is *higher* than the experimental result, the ratio $\bar{d}/\bar{u}$ should decrease. This is consistent with the information from the absolute measurement of proton-proton and proton-deuteron cross-sections. It is interesting to note that the $\bar{d}$ distribution function almost coincides for DIS PDFs [3] and MRST PDFs [1], whereas the $\bar{u}$ distribution function from the DIS fit is smaller than the one obtained by MRST. This is not accidental, since MRST includes the E-866 data in their fit. While the preceding discussion indicates how sea quark distributions are influenced by the DY data, it is less obvious that gluon PDFs at large values of x may also be affected. To see that this may happen, recall that the contribution of the qg partonic subprocess to the dimuon production cross-section is relatively large, approximately 15% of the total, and *negative*. Decreasing the gluon content of the proton may therefore increase the rapidity distribution. A similar effect can be achieved by increasing sea quark distributions. Since both gluon and sea PDFs at large x are poorly constrained by the DIS fit, the impact of the DY data on each of these distributions can not be disentangled using qualitative considerations.

Following the discussion in this section, we include the E-605 data and the E-866 data on the ratio of deuteron to proton cross-sections in the combined DIS/DY fit. These two data sets improve the precision of sea quark distributions obtained from the DIS fit in two different ways. The E-605 data improves the precision of sea quark distributions for $x \gtrsim 0.2$ in a "flavor-blind" fashion, whereas $\bar{u} - \bar{d}$ for $x \gtrsim 0.1$ is constrained by the E-866 data. Note that even if the E-866 and E-772 measurements of the absolute proton and deuteron cross-sections were consistent with the DIS data, they could not have added much new information compared to the DY data which we include in the fit. This is because at small rapidities the E-605 data is as good as the E-866 and E-772 data, while at large rapidities the PDFs are already constrained by the DIS data. We conclude that our selection of the DY data is sufficiently representative and can be combined with the DIS data to determine parton distribution functions with high precision. We describe the results of the combined fit in the next Section.

III. A FIT TO THE COMBINED DIS AND DY DATA

A. Theoretical input

In this Section we fit PDFs to both the DIS and DY data. We begin with a brief description of the salient features of

the approach in Ref. [3]. We use the following parameterization of parton distribution functions at $Q_0^2 = 9$ GeV^2:

$$xq_{\mathrm{V}}(x, Q_0) = \frac{2\delta_{qu} + \delta_{qd}}{N_q^{\mathrm{V}}} x^{a_q}(1-x)^{b_q} x^{P_{q,\mathrm{V}}(x)},$$
$$P_{q,\mathrm{V}} = \gamma_{1,q}x + \gamma_{2,q}x^2, \qquad q = u, d; \tag{3}$$

$$xq_{\mathrm{S}}(x, Q_0) = A_q x^{a_{qs}}(1-x)^{b_{qs}} x^{P_{q,s}(x)},$$
$$P_{q,\mathrm{s}} = \gamma_{1,qs}x, \qquad q = u, d, s; \tag{4}$$

$$xG(x, Q_0) = A_{\mathrm{G}}x^{a_{\mathrm{G}}}(1-x)^{b_{\mathrm{G}}} x^{P_{\mathrm{G}}(x)}, \qquad P_{\mathrm{G}} = \gamma_{1,\mathrm{G}}x. \tag{5}$$

Valence quark distributions are displayed in Eq. (3), sea quarks are shown in Eq. (4), and gluons are shown in Eq. (5). To obtain PDFs at arbitrary Q^2, we employ the DGLAP evolution equation with the NNLO Altarelli-Parisi splitting kernels computed recently [6]. The PDF parameterization in Eqs. (3)–(5) differs from the one in Ref. [3]. It allows more flexibility, which is important since more data are included in the fit. Note that some parameters in Eqs. (3)–(5) are interdependent. For valence quarks, N_V^q is calculated from the requirement that the total numbers of valence u and d quarks are two and one, respectively. Also, the normalization of the gluon distribution, A_{G}, is related to the other parameters through the momentum conservation constraint. Since the strange quark distribution is not well constrained by the data used in the fit, we fix it using the CCFR data on dimuon production in neutrino-nucleon collisions [14]. This leads to $A_s = 0.08$, $b_{ss} = 7$, and $\gamma_{1,ss} = 0$. We also set $a_{us} = a_{ds} = a_{ss}$ which is a natural choice since the existing DIS/DY data is not useful for detecting nonuniversality of sea PDFs at small x. The contribution of heavy quarks to DIS structure functions is accounted for within the massive factorization scheme using the one-loop computations of Ref. [15]. For the fixed-target DY data employed in the fit, heavy quark contributions are unimportant.

The DIS deuteron data are corrected for nuclear effects that include Fermi motion, shadowing and nucleon off-shellness. Since the deuteron nuclear correction increases with x, the cut $x < 0.75$ was applied to the DIS deuteron target data in Ref. [3]. Because uncertainties in nuclear effects at large x are now better understood [16], we do not apply a similar cut in the current analysis and include the DIS data points up to $x = 0.9$, the largest value of x available in the existing DIS data. The DY data are not corrected for nuclear effects since these data points are concentrated at $x \lesssim 0.3$, where nuclear corrections are small [17].

Our treatment of power corrections to logarithmic evolution of the DIS structure functions follows Refs. [3,18]. We suppress the sensitivity of the structure functions to powerlike terms by removing the DIS data with $Q^2 < 2.5$ GeV^2 and hadronic invariant mass $W < 1.8$ GeV. For the remaining data, target mass corrections important at

TABLE I. The number of data points (NDP) and values of χ^2/NDP for each experiment used in the fit.

Experiment	NDP	χ^2/NDP	Experiment	NDP	χ^2/NDP
SLAC-E-49A	118	0.56	BCDMS	605	1.10
SLAC-E-49B	299	1.18	NMC	490	1.26
SLAC-E-87	218	0.94	H1(96-97)	135	1.13
SLAC-E-89A	148	1.42	ZEUS(96-97)	161	1.28
SLAC-E-89B	162	0.80	FNAL-E-605	119	1.49
SLAC-E-139	26	1.03	FNAL-E-866	39	1.13
SLAC-E-140	17	0.47	Total	2537	1.13

large x are applied using the Georgi-Politzer scheme [19]. Applying just the target mass corrections is insufficient. We must also add twist-4 terms to the DIS structure functions. These terms are parameterized by cubic spline polynomials of x whose coefficients are fitted to data. Note that twist-4 contributions produce only $\sim 10\%$ corrections to DIS PDFs even for $Q^2 \sim 2.5$ GeV^2 and become unimportant for $Q^2 \sim 20$ GeV^2. By analogy, since the DY data employed in our analysis correspond to $Q^2 \geq 25$ GeV^2, we do not consider power corrections to this part of the data sample.

B. Results of the fit

The PDF parameters in Eqs. (3)–(5) and the coefficients of the twist-4 corrections to the DIS structure functions are obtained from the fit to the DIS data for proton and deuteron targets [20] and the DY data of Refs. [7,10]. They are shown in Table II. To check that our PDF parameterization is sufficiently flexible, we modified the polynomials $P_{q,G}(x)$ in Eqs. (3)–(5) by adding terms of the type $\gamma_n x^n$, $n = 2, 3$ for the sea, gluon and valence distributions. We found that such modifications do not improve the description of the data. The overall quality of the fit is good; for its final version the value $\chi^2/\text{NDP} = 2862/2537 = 1.13$ is obtained.

To demonstrate the quality of the fit in more detail, we show values of χ^2/NDP for separate experiments in Table I. It is clear from the Table that the description of the data is acceptable. In Fig. 5 results for the pulls of the DY data used in the fit are displayed. They do not demonstrate any systematic trend. The description of the E-605

data has randomly distributed deviations that can be attributed to fluctuations beyond quoted experimental errors. We can model the possibility of some experimental errors being underestimated by rescaling the errors for experiments with $\chi^2/\text{NDP} > 1$. We find that these scale factors do not exceed 1.2 and the impact of the rescaling on the PDF errors is within 20%.

Having established that the combined DIS/DY fit leads to an acceptable description of the data, we discuss the major differences between the DIS/DY and DIS PDFs. For this comparison, the DIS PDFs were recalculated using the parameterizations shown in Eqs. (3)–(5). Hence, the comparison presented below illustrates the differences in PDFs caused by the inclusion of the fixed-target Drell-Yan data into the fit.

As we discussed in Sec. II, we expect sea quark distributions at large values of x to be mostly affected by the DY data. This is indeed what happens, as shown in Fig. 6. Both the symmetric and antisymmetric combinations of $\bar{u}$ and $\bar{d}$ distributions are displayed. Dramatic improvements in the precision for large values of x are observed once the DY data are included in the fit. For $x \lesssim 0.1$, the impact of the DY data on the isospin-symmetric combination $x(\bar{u} + \bar{d})$ is marginal, whereas the precision of the combination $x(\bar{d} - \bar{u})$ in the DIS/DY fit is higher for $x > 0.02$. The central values of the sea quark distributions obtained in the DIS/DY and DIS fits agree within the errors, indicating consistency between the DIS and DY data. The largest discrepancies are at the level of 1 standard deviation; they occur at small x, where the DIS and DY data have comparable precision.

A better separation of sea and valence quark distributions in the DIS/DY fit leads to an increased precision of quark distributions, as shown in Fig. 7. The effect is more pronounced for the d-quark content of the proton. Both the u- and d- distributions obtained in the DIS/DY fit are smaller than similar distributions in the DIS fit at moderate values of x, but the difference is about 1σ. The gluon distribution is practically unaffected by the DY data used in the fit, as seen in Fig. 7.

The theoretical errors of the DIS/DY PDFs due to variations of the renormalization and factorization scales do not exceed the "experimental" errors obtained by propagating statistical and systematic uncertainties in the data.

TABLE II. Parameters of parton distribution functions derived from the NNLO QCD fit to the DIS and DY data. The errors on fit parameters are obtained by propagating the statistical and systematic errors in the data. As described in the text, a_{u_s} and a_{d_s} are identical by construction.

	u_v	d_v	u_s	d_s	g
a	0.670 ± 0.035	0.61 ± 0.12	-0.2182 ± 0.0044	-0.2182 ± 0.0044	-0.198 ± 0.015
b	3.639 ± 0.077	5.21 ± 0.42	6.14 ± 0.25	8.24 ± 0.40	5.41 ± 0.13
γ_1	-0.41 ± 0.27	0.18 ± 0.27	1.04 ± 0.32	-1.97 ± 0.48	2.09 ± 0.94
γ_2	-0.91 ± 0.18	-4.19 ± 0.18			
A			0.1488 ± 0.0060	0.1220 ± 0.0063	
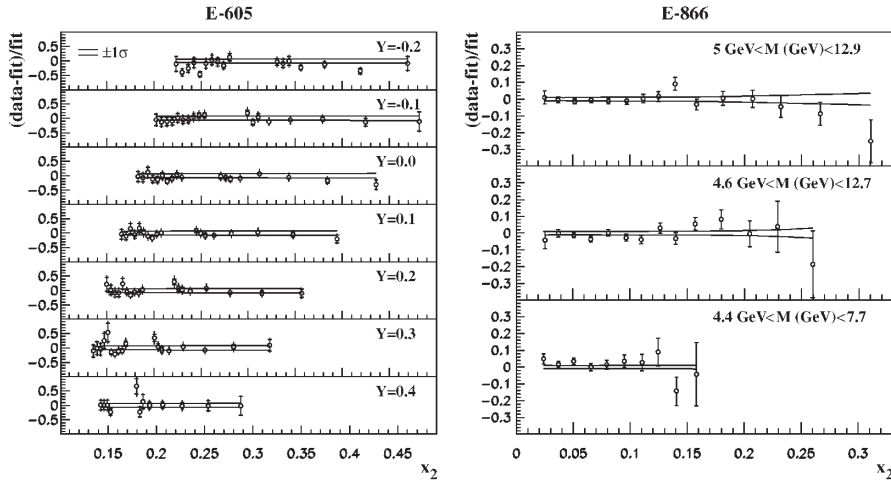
FIG. 5.   Data points used in the DIS/DY fit vs predictions based on fitted PDFs. The bands reflect the 1σ uncertainty of fitted PDFs.
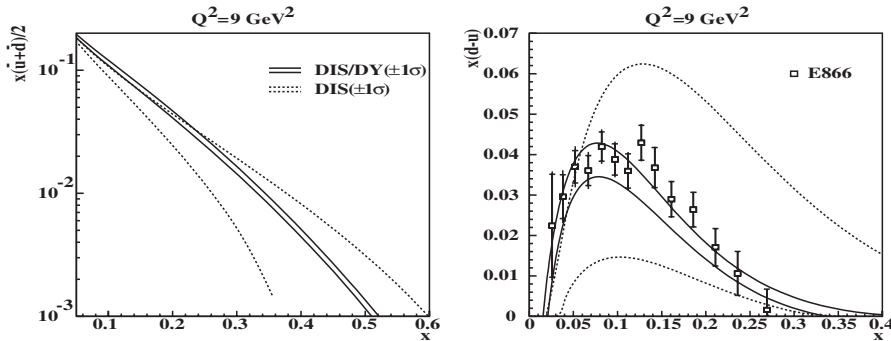
FIG. 6.   The 1σ bands for isospin-symmetric and antisymmetric sea quark distributions from the DIS/DY (solid) and DIS (dashes) fits.

The theoretical uncertainties have the largest impact on the isospin-symmetric combination of sea quark distributions, where the theoretical and experimental errors are comparable for $x \gtrsim 0.3$; this is shown in Fig. 8. The DIS/DY fit constrains nonstrange sea quark distributions with a precision better than $\pm 30\%$ for $x \sim 0.7$. The NNLO QCD corrections to the DY process are crucial for achieving this precision. If the NLO QCD theoretical prediction for

the DY rapidity distribution is used in the fit, the theoretical uncertainty due to the renormalization scale variation is a factor of 2 larger than in the NNLO fit; as shown in Fig. 8, it exceeds experimental errors in the isospin-symmetric sea distribution at large values of x.

The similar error estimated in the CTEQ fit [2] is an order of magnitude larger, as shown in Fig. 8. One of the reasons for this disagreement is that in the CTEQ analysis,
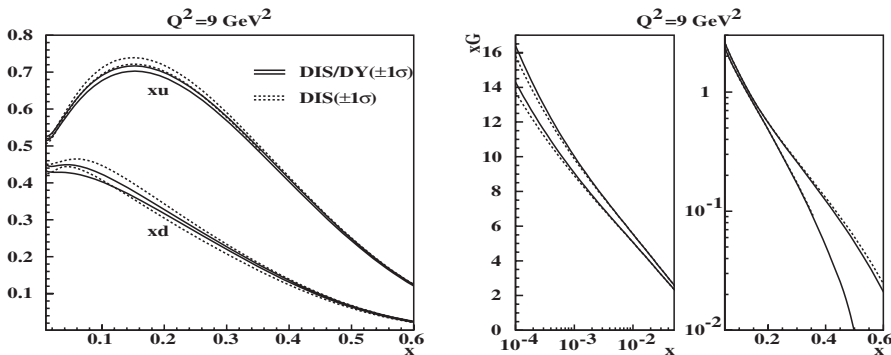
FIG. 7.   The same as in Fig. 6 for up (down) quarks and gluons.
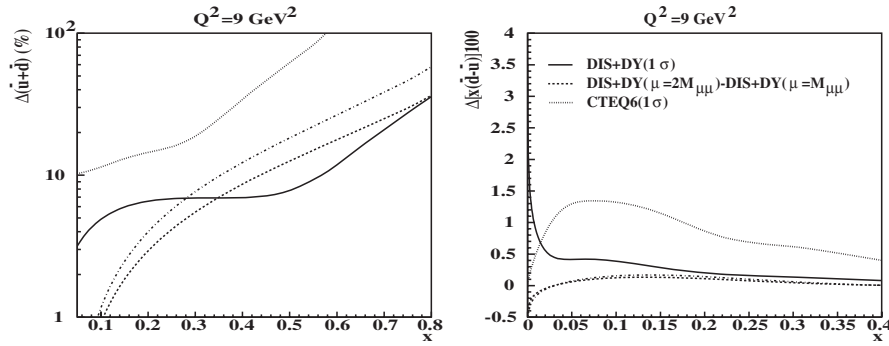
FIG. 8. The 1σ errors on the isospin-symmetric and antisymmetric sea quark distributions due to uncertainties in data. The results of the current analysis (solid) are compared to that of the CTEQ collaboration (dots) and to the uncertainties due to variations of the renormalization ans factorization scales (dashes). The latter quantity with the DY cross-section calculated through NLO in perturbative QCD is also given for comparison (dot-dashes).

the criterion $\Delta\chi^2 = 100$ is applied to account for possible inconsistencies in the data. In our case, good data consistency is a prerequisite for assembling the data sample. Hence, we apply the standard criterion $\Delta\chi^2 = 1$ that allows us to use the full power of the statistical analysis in our PDF determination.

C. Phenomenological implications

In this Section we briefly discuss some phenomenological implications of the above analysis. A broad measure of the consistency of PDFs with other observables is provided by the value of the strong coupling constant $\alpha_s(M_Z)$. The strong coupling constant obtained in the DIS/DY fit, $\alpha_s(M_Z) = 0.1128(15)$, agrees with the value obtained in the DIS fit of Ref. [3] within errors. It is interesting that PDF fits generally prefer *smaller* values of the strong coupling constant than the current world average value $\alpha_s(M_Z) = 0.1176(20)$ [21], and that the inclusion of NNLO corrections into the fits makes the disagreement *larger* (see also the recent results of Ref. [22]).

Another interesting observable to discuss is the Pascos-Wolfenstein ratio. Recently, the NuTeV collaboration measured the Weinberg angle in neutrino-nucleon scattering [23] and observed an anomaly. The significance of this anomaly is still an open issue since its interpretation depends on subtle details of the quark structure of the nucleon and on the correct application of QCD and electroweak radiative corrections [24]. While discussing these issues is beyond the scope of this paper, we would like to illustrate briefly the importance of improving PDFs at large values of x for the NuTeV analysis.

For the sake of illustration, we consider the Pascos-Wolfenstein ratio

$$R^- = \frac{\sigma_{NC}^{\nu} - \sigma_{NC}^{\bar{\nu}}}{\sigma_{CC}^{\nu} - \sigma_{CC}^{\bar{\nu}}} \approx \frac{1}{2} - \sin^2\theta_W. \qquad (6)$$

Although the NuTeV collaboration does not measure this ratio directly, we assume that R^- is extracted from the data

and is used to determine the Weinberg angle. The simple relation between R^- and $\sin^2\theta_W$ in Eq. (6) is only valid for an isoscalar target. Since the iron target used by NuTeV is not isoscalar, there is a correction to the Pascos-Wolfenstein ratio [25]

$$\delta R^- \approx \frac{2Z - A}{A}\left(\frac{x_1^-}{x_0^-}\right)\left(1 - \frac{7}{3}\sin^2\theta_W\right), \qquad (7)$$

where A and Z are the target atomic weight and charge and

$$x_{0,1}^- = \int_0^1 dx\, x(u_{\mathrm{val}} \pm d_{\mathrm{val}}). \qquad (8)$$

For iron, δR^- is a factor of 10 larger than the NuTeV experimental error; hence the ratio x_1^-/x_0^- must be known to better than 10%. For the DIS/DY PDFs obtained in this paper, the value of x_1^-/x_0^- at $Q^2 = 20$ GeV^2 is 0.4459 ± 0.0094. The DIS/DY PDFs therefore suppress the errors in the determination of $\sin^2\theta_W$ due to the nonisoscalarity of NuTeV target to an acceptable value. We stress that inclusion of the DY data into the fit is crucial for achieving this accuracy. For example, in the NNLO DIS fit of Ref. [3] the value $x_1^-/x_0^- = 0.4324 \pm 0.0281$ at $Q^2 = 20$ GeV^2 was obtained. In the global NLO fits by the CTEQ and MRST collaborations, these values are 0.4197 ± 0.0307 and 0.4317 ± 0.0204, respectively.

The production of Z and W bosons at hadron colliders can be used to measure partonic luminosities [26]. In Fig. 9, the NNLO QCD predictions for these rates calculated using the DIS/DY PDFs and DIS PDFs of Ref. [3] and the coefficient functions of Ref. [27] are compared to recent Tevatron results [28]. The errors in the theoretical predictions arise from experimental uncertainties in the data used in the PDF fit; additional uncertainties come from varying the normalization factor A_s in Eq. (4) by 40% and from varying the charm quark mass by 20%. Given the experimental errors on the Z and W production cross-sections, the theoretical predictions agree with the
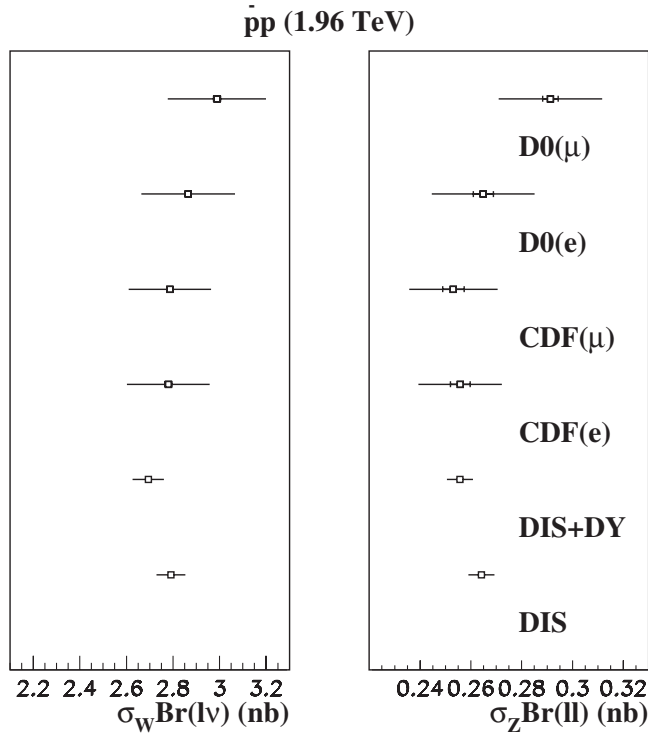
FIG. 9. The preliminary Run II data for the W and Z production rates measured at the Tevatron. The NNLO theoretical predictions predictions are obtained with the DIS/DY PDFs and the DIS PDFs of Ref. [3].

IV. CONCLUSIONS

In this paper we extend the NNLO QCD analysis of proton PDFs performed in Ref. [3] by including fixed-target Drell-Yan data into the fit. The possibility to do so without compromising the precision is due to the computation of the dilepton rapidity distribution in the DY process through NNLO in QCD [12,13]. When assembling the data sample, we pay particular attention to the consistency of the DIS and DY data. We find that the DY data does not agree with the DIS data for large dilepton rapidities; the disagreement actually becomes worse when the NNLO QCD corrections to the DY cross sections are taken into account. For this reason, we only include the E-605 data and the E-866 data on the ratio of proton and deuteron cross-sections in the combined DIS/DY fit.

We find that the DY data improves the precision of sea quark PDFs at large values of x, $x \gtrsim 0.1$. The overall quality of the DIS/DY fit is good, with $\chi^2/\mathrm{NDP} = 1.13$. The differences between the DIS/DY PDFs obtained in this paper and the DIS PDFs derived in Ref. [3] do not exceed 1 standard deviation, demonstrating good consistency of the data.

measured rates. The theory results obtained with the DIS/DY and DIS PDFs agree within 1 standard deviation, demonstrating good stability of the fits with respect to the selection of data.

[1] A. D. Martin, R. G. Roberts, W. J. Stirling, and R. S. Thorne, Eur. Phys. J. C **23**, 73 (2002).

[2] J. Pumplin, D. R. Stump, J. Huston, H. L. Lai, P. Nadolsky, and W. K. Tung, J. High Energy Phys. 07 (2002) 012.

[3] S. I. Alekhin, Phys. Rev. D **68**, 014002 (2003); S. Alekhin, Pis'ma Zh. Eksp. Teor. Fiz. **82**, 710 (2005) [JETP Lett. **82**, 628 (2005)].

[4] D. I. Kazakov and A. V. Kotikov, Phys. Lett. B **291**, 171 (1992); W. L. van Neerven and E. B. Zijlstra, Phys. Lett. B **272**, 127 (1991); **273**, 476 (1991); **297**, 377 (1992).

[5] A. Retey and J. A. Vermaseren, Nucl. Phys. **B604**, 281 (2001).

[6] S. Moch, J. A. M. Vermaseren, and A. Vogt, Nucl. Phys. **B688**, 101 (2004); A. Vogt, S. Moch, and J. A. M. Vermaseren, Nucl. Phys. **B691**, 129 (2004).

[7] G. Moreno *et al.*, Phys. Rev. D **43**, 2815 (1991).

[8] P. L. McGaughey *et al.*, Phys. Rev. D **50**, 3038 (1994).

[9] J. C. Webb *et al.*, hep-ex/0302019.

[10] R. S. Towell *et al.*, Phys. Rev. D **64**, 052002 (2001).

[11] G. Altarelli *et al.*, Nucl. Phys. **B157**, 461 (1979).

[12] C. Anastasiou, L. Dixon, K. Melnikov, and F. Petriello, Phys. Rev. Lett. **91**, 182002 (2003).

[13] C. Anastasiou, L. Dixon, K. Melnikov, and F. Petriello, Phys. Rev. D **69**, 094008 (2004).

[14] A. O. Bazarko *et al.* (CCFR Collaboration), Z. Phys. C **65**, 189 (1995).

[15] E. Laenen, S. Riemersma, J. Smith, and W. L. van Neerven, Nucl. Phys. **B392**, 229 (1993).

[16] S. A. Kulagin and R. Petti, Nucl. Phys. A **765**, 126 (2006).

[17] D. M. Alde *et al.*, Phys. Rev. Lett. **64**, 2479 (1990).

[18] S. I. Alekhin, S. A. Kulagin, and S. Liuti, Phys. Rev. D **69**, 114009 (2004).

[19] H. Georgi and H. D. Politzer, Phys. Rev. D **14**, 1829 (1976).

[20] L. W. Whitlow, E. M. Riordan, S. Dasu, S. Rock, and A. Bodek, Phys. Lett. B **282**, 475 (1992); A. C. Benvenuti

et al. (BCDMS Collaboration), Phys. Lett. B **223**, 485 (1989); **237**, 592 (1990); M. Arneodo *et al.* (New Muon Collaboration), Nucl. Phys. **B483**, 3 (1997); C. Adloff *et al.* (H1 Collaboration), Eur. Phys. J. C **21**, 33 (2001); S. Chekanov *et al.* (ZEUS Collaboration), Eur. Phys. J. C **21**, 443 (2001).

[21] S. Eidelman *et al.*, Phys. Lett. B **592**, 1 (2004).

[22] J. Blumlein, H. Bottcher, and A. Guffanti, Nucl. Phys. B, Proc. Suppl. **135**, 152 (2004).

[23] G. P. Zeller *et al.* (NuTeV Collaboration), Phys. Rev. Lett. **88**, 091802 (2002); **90**, 239902(E) (2003).

[24] S. Davidson, S. Forte, P. Gambino, N. Rius, and A. Strumia, J. High Energy Phys. 02 (2002) 037; K. S. McFarland and S. O. Moch, hep-ph/0306052; S. Kretzer, F. Olness, J. Pumplin, D. Stump, M. H. Reno, and W. K.

Tung, Phys. Rev. Lett. **93**, 041802 (2004); R. K. Ellis and B. Dobrescu, Phys. Rev. D **69**, 114014 (2004); K.-P. O. Diener, S. Dittmaier, and W. Hollik, Phys. Rev. D **69**, 073005 (2004); A. D. Martin, R. G. Roberts, W. J. Stirling, and R. S. Thorne, Eur. Phys. J. C **39**, 155 (2005); M. Glück, P. Jimenez-Delgado, and E. Reya, Phys. Rev. Lett. **95**, 022002 (2005).

[25] S. A. Kulagin, Phys. Rev. D **67**, 091301 (2003).

[26] M. Dittmar, F. Pauss, and D. Zurcher, Phys. Rev. D **56**, 7284 (1997).

[27] R. Hamberg, W. L. van Neerven, and T. Matsuura, Nucl. Phys. **B359**, 343 (1991); **B644**, 403(E) (2002); R. V. Harlander and W. B. Kilgore, Phys. Rev. Lett. **88**, 201801 (2002).

[28] A. M. Bellavance, hep-ex/0506025.